Covalent or not? Energy decomposition analysis of metal–metal bonding in alkaline-Earth dimetallocene complexes

ARTICLE *in* JOURNAL OF MOLECULAR STRUCTURE THEOCHEM · JANUARY 2009

Impact Factor: 1.37 · DOI: 10.1016/j.theochem.2008.10.004

1 AUTHOR:

Yu-He Kan
Huaiyin Normal University
137 PUBLICATIONS **1,050** CITATIONS

SEE PROFILE

Journal of Molecular Structure: THEOCHEM 894 (2009) 88–92

Contents lists available at ScienceDirect

Journal of Molecular Structure: THEOCHEM

journal homepage: www.elsevier.com/locate/theochem

Covalent or not? Energy decomposition analysis of metal–metal bonding in alkaline-Earth dimetallocene complexes

Yu-He Kan *

Department of Chemistry, Huaiyin Teachers College, Jiangsu Province Key Laboratory for Chemistry of Low-Dimensional Materials, No. 111, Changjiang West Road, Huaian, Jiangsu 223300, China

ARTICLE INFO

Article history:
Received 27 June 2008
Received in revised form 4 October 2008
Accepted 6 October 2008
Available online 17 October 2008

Keywords:
Metallocenes
Alkaline-Earth metals
Energy decomposition analysis
Metal–metal bonding

ABSTRACT

The geometries, metal–metal bond dissociation energies of Group 2 dimetallocene complexes $M_2(\eta^5\text{–}C_5H_5)_2$ (M = Be, Mg, Ca, Sr and Ba) have been calculated using density functional theory at the BP86 level with TZ2P basis sets. The nature of metal–metal bonding has been analyzed with an energy decomposition method. The results revealed that the M–M binding interactions in these nonpolar bonding alkaline-Earth metal complexes have more ionic character than covalent character, rather than the sole covalent bond. Molecular orbital calculations indicate that, for the heavier alkaline-Earth metal (Ca, Sr and Ba) compounds, substantial $(n-1)d$ character is found in the δ bonding between metal and cyclopentadiene (Cp) ring, while there is few δ bonding interaction between M–M bond due to longer M–M bond distance.

1. Introduction

During the last two decades the metallocenes chemistry of the main-group elements has experienced remarkable development. A large number of main-group metallocenes compounds with elements of the Groups 1, 2, 13, 14 and 15, have been synthesized and structurally characterized and the main principles of structure, bonding and reactivity are well understood [1–4]. Otherwise, following the report on the synthesis and structure of an unprecedented dimetal core cyclopentadienyl (Cp) compound $[Zn_2(\eta^5\text{–}C_5Me_5)_2]$ [5], dimetallocene has arisen more attentions quickly. The unique nature of this compound has motivated an astonishingly large number of both experimental and theoretical investigations [6–16]. The alkaline-Earth metal metallocenes are an especially attractive family of metallocenes [17,18]. Carmona et al. review recent developments in the chemistry of beryllocenes [19]. The energy decomposition analysis (EDA) of the interactions suggests that the bonding between metal and cyclopentadienyl ligand in the alkaline-Earth metallocenes is mainly caused by electrostatic forces [20]. For the dimetallocene, a theoretical study of the analogous model compounds $[M_2(C_5H_5)_2]$ (M = Be, Mg, Ca) has been reported by Xie et al. [21]. Just recently, Merino et al. theoretically predicted geometries and stabilities of the multimetallocenes CpM_nCp compounds and investigated the metal–Cp interactions using EDA method [22]. Moreover, Green et al. reported some novel thermally stable Mg(I) compounds and revealed that central Mg^{2+} units that have single covalent Mg–Mg bonding interactions [23]. We have analyzed the bonding in Group 12 transition metallocenes, the EDA result indicates metal–metal bonds have slightly more attractive contributions from classical electrostatic interactions than the attractive orbital interactions [24]. In this letter we present results for the alkaline-Earth metals (+1 oxidation state) metallocenes $[M_2(Cp)_2]$ (M = Be–Ba,) by EDA and electron localization function (ELF). Detailed theoretical calculations aimed to shed some light on the nature of the metal–metal bonding in these systems.

2. Theoretical methods

Energies and geometries were calculated using the generalized gradient approximation (GGA) of DFT at the BP86 level. GGA proceeds from the local density approximation (LDA) where exchange is described by Slater's Xα potential and correlation is treated in the Vosko–Wilk–Nusair (VWN) parametrization. Scalar relativistic effects have been considered using the zero-order regular approximation (ZORA) [25]. The basis sets used are of triple-ζ quality augmented by two sets of polarization functions (TZ2P), and a frozen-core approximation was not used. To assure the usage of ground-state geometries in all calculations, the Hessian matrix was checked for the absence of imaginary entries.

The bonding interactions between the two equal metal fragments have been analyzed by means of the energy decomposition analysis implemented in ADF package, which is based on the EDA method of Morokuma and the extended transition state (ETS) partitioning scheme developed by Ziegler and Rauk. The overall bond

* Fax: +86 517 83525369.
E-mail address: yhkan@yahoo.cn

0166-1280/$ - see front matter © 2008 Elsevier B.V. All rights reserved.
doi:10.1016/j.theochem.2008.10.004

energy ΔE can be determined from interaction energy (ΔE_{int}) and the fragment preparation energy ΔE_{prep}, the instantaneous ΔE_{int} between the two fragments can be divided into three main components [Eq. (1)], details about EDA can be found in the literature [26].

$$\Delta E_{int} = \Delta E_{Pauli} + \Delta E_{elstat} + \Delta E_{orb} \quad (1)$$

The bonding properties of the dimetallocene have also been studied according to topological analysis of the ELF [27], which is a robust descriptor of chemical bonding based on topological analyses of local quantum mechanical functions related to the Pauli exclusion principle.

All calculations were performed using the Amsterdam Density Functional (ADF 2006.01) program [26]. The topological analysis of ELF has been performed using the DGrid programs[28].

3. Results and discussion

3.1. Geometric structures

The calculation of the vibrational frequencies revealed that all structures are minima on the potential energy surface (PES), which has D_{5h} symmetry. Table 1 gives the calculated most important structural parameters of the investigated metallocenes. Apparently, the M–M and M–C bond distance in the D_{5h} symmetric $C_5H_5M–MC_5H_5$ increase descending the periodic table from Be to Ba. However, the C–C bond distance in Cp ligand does not change much and amounts to ca. 1.42 Å throughout the series. This agrees satisfactorily with previous theoretical work [21,22], which also yield a monotonic increase of the M–M and C–M bond along $Be_2(Cp)_2$, $Mg_2(Cp)_2$ and $Ca_2(Cp)_2$, while the M–M value presented here is somewhat larger than the previous result by 0.004–0.089 Å. The calculated bond parameters which are given here should be more reliable, because, the calculated structure is in agreement with discussion of the experimental structure for $Be(Cp)_2$ at similar BP86/TZP level [20] and the higher quality of the basis sets used in this work. Furthermore, in our recent work, the calculated Zn–Zn distance (2.306 Å) is in excellent agreement with the experimental values (2.305 Å) for $Zn_2(\eta^5–C_5Me_5)_2$ use the same method [24]. It should be noted, for Ca compound, Merino et al. [22] obtain Ca–Ca of 3.961 Å with same level, but the result is different from the present ones of 3.823 Å. Calculation of the vibrational frequencies at the Ca–Ca of 3.961 Å geometry shows that it is not minima on the potential energy surface with an imaginary frequency of $-11.6\ cm^{-1}$. Moreover, Westerhausen et al. give a BP86/TZVPP Ca–Ca of 3.806 Å [29], rather close to the result of this work.

To the best of our knowledge, the complexes with M = Sr and Ba have not been calculated by *ab initio* or DFT methods before. Thus, the data in Table 1 are the first complete set of theoretically predicted geometries of Group 2 transition dimetallocenes. The comparison of the alkaline-Earth dimetallocene $M_2(Cp)_2$ with the metallocene species $Be(Cp)_2$ –$Ba(Cp)_2$ shows same trend of metal and Cp ligand geometrical parameters. With the increase of atom radii, the M–M and M–C bond elongate substantially by 0.3–0.7 Å and 0.1–0.4 Å from Be to Ba, respectively. These M–M distances are much shorter than the experimental value for the weakly bound diatomic M_2 (M–M = 2.45, 3.597, 4.707 Å along Be, Mg and Ca) [21], indicating the cyclopentadienyl groups strengthen the M–M bonding than that for the metal dimer. This reveals there are comparable M–M bonding interactions in all of these dimetallocene compounds. In order to investigate the nature of M–M bonding in these metallocenes, in the following section we will do this in a quantitative way by using the results of molecular orbital and the energy decomposition analysis [26].

3.2. Fragment orbital (FO) and ELF analysis

The bonding situation in alkaline-Earth monometallocenes $M(Cp)_2$ (M = Be–Ba) compounds has been analyzed with qualitative bonding models [2,4]. Recent calculation analysis showed that the bonding of the Cp ligand to the alkaline-Earth elements is considered to be predominantly ionic [20,30]. In this work, we focus on nature of the metal–metal bonding derives from FO calculation of the orbital interaction in all alkaline-Earth dimetallocenes $M_2(Cp)_2$. Fig. 1 shows a qualitative orbital correlation diagram for the formation of MOs in $Be_2(\eta^5–C_5H_5)_2$ using the fragment $Be(\eta^5–C_5H_5)$.

The results of Kohn–Sham MO analysis indicate that the Be–Be bonding interaction mainly resides in the HOMO, and same results can be found in Mg compound. The bonding interaction mainly comes from the <*ns*|*ns*> bond overlap between two *n*s singly occupied molecular orbitals (SOMO) in M_2Cp_2 (see Fig. 1). The fragment orbital calculations reveal that it has a contribution of $6a_1$ orbitals in fragment $Be(\eta^5–C_5H_5)$ close to 97%, the metal–metal bond involves mostly the Be 2s orbitals (more than 78%) and $2p_z$ orbitals of 22%. In Mg complex, the bonding HOMO comes from combination of two $8a_1$ fragment orbital which is about 98%, there are still two principal bonding components: 82% 3s orbitals and 17% $3p_z$ orbitals from Mg. This is comparable with that calculated for the novelly stable MgMg bond compound, $\{Mg[(Ar'N)_2C(NMe_2)]\}_2$ (Ar′ is $C_6H_3Me_2$-2,6) (93.2% s-, 6.0% p-character), which has a different ligands [23]. Note that the relative contribution in the remaining heavier alkaline-Earth complexes shows the different

Table 1
BP/TZ2P calculated values of the optimized geometrical parameters of investigated compounds (bond length *R* in angstrom, bond angle θ in degree).

	Method	*R*(M–M)	*R*(M–C)	*R*(C–C)	θ(M–M–C)	Ref.
CpBeBeCp	BP86/TZ2P	2.081	1.979	1.422	142.2	This work
	BP86/TZ2P	2.077	1.966	1.421	142.1	[22]
	B3LYP/DZP	2.057	1.968	1.425		[21]
	BP86/DZP	2.066	1.972	1.434		[21]
CpMgMgCp	BP86/TZ2P	2.790	2.378	1.422	149.4	This work
	BP86/TZ2P	2.809	2.376	1.424	149.4	[22]
	B3LYP/DZP	2.766	2.376	1.428		[21]
	BP86/DZP	2.786	2.378	1.436		[21]
CpCaCaCp	BP86/TZ2P	3.823	2.659	1.422	153.0	This work
	BP86/TZ2P	3.961	2.661	1.421	153.0	[22]
	B3LYP/DZP	3.740	2.668	1.425		[21]
	BP86/DZP	3.734	2.655	1.433		[21]
CpSrSrCp	BP86/TZ2P	4.171	2.805	1.420	154.5	This work
CpBaBaCp	BP86/TZ2P	4.662	2.953	1.430	155.9	This work

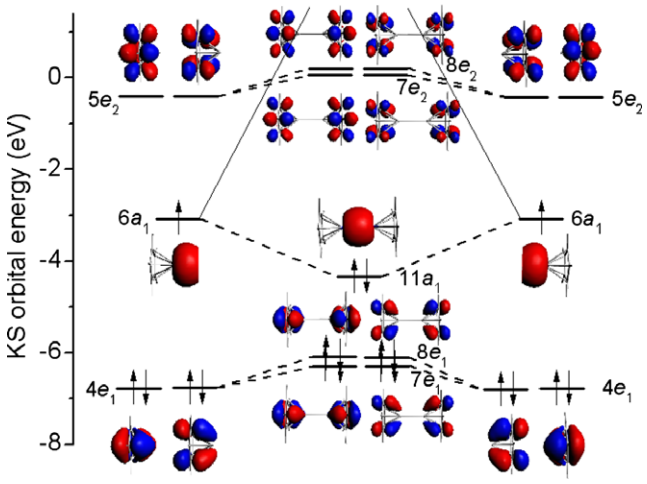

Fig. 1. Qualitative orbital diagram for the formation of $Be_2(\eta^5\text{–}C_5H_5)_2$ from the fragment $Be(\eta^5\text{–}C_5H_5)$.

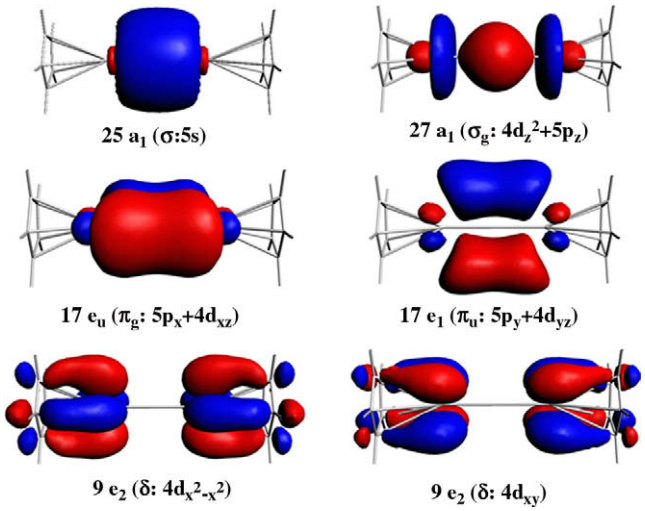

Fig. 2. Some bonding σ, π and δ molecular orbitals in $Sr_2(\eta^5\text{–}C_5H_5)_2$ at the BP86/TZ2P level.

results from Be and Mg species. In case of $Ca_2(\eta^5\text{–}C_5H_5)_2$, the bonding HOMO mainly comes from combination of two $10a_1$ fragment orbital which is about 93%, in addition, a sizable contribution of 7% from $11a_1$ fragment orbital. A molecular orbital analysis of the fragments indicates that $10a_1$ fragment orbital is composed of about 90% 4s orbital and about 11% $4p_z$ orbitals. It is worth noting that, there is considerable $3d_z^2$ orbital of about 74% in $11a_1$ orbital, besides 24% $4p_z$ orbital. Introduction of the first subvalence d shell, i.e., 3d orbital, has relatively a little effect on the spatial extent of the *ns* AO. For Sr and Ba species, we also find marginal contributions of the metal $(n-1)d_z^2$ AO. To validate the result, the calculations were also carried out with other STO basis sets, including basis set of near limit in ADF, QZ4P basis set. As seen from Table 2, three basis sets give closely similar results. Beside the d_z^2 in HOMO, for Ca, Sr and Ba compounds, there are substantial $(n-1)d$ characters (d_{xz}, $d_{x^2-y^2}$ and d_{xy}) in some unoccupied frontier orbitals of alkaline-Earth metals. These substantial d characters form π and δ bonding MOs, which are markedly weaker than σ bonding from *ns* and $(n-d)d_z^2$. Take Sr compound as an example, some typical bonding MOs are listed in Fig. 2. Interestingly, metal forms preferential δ bonds with the Cp ring, while there is few δ bonding interaction between M–M bond because of too longer M–M bond distance. The EDA orbital decomposition of M–M bonding support this result (vide infra). Gagliardi and Pyykkö [31] have proved that there are multiple bond between Ba and N ring with a substantial 5d Ba character in some alkaline-Earth metal sandwich compounds. Similiarly, along group 2 series, the d character of the δ MOs is increased on alkaline-Earth metal.

Fig. 3 displays the localization domains of the $Be_2(\eta^5\text{–}C_5H_5)_2$ complex which is representative of the whole series. The picture clearly shows the presence of a V(M,M) disynaptic basin. The local ELF maximum on the atom–atom vector characterizes the formation of a single bond between two metal atoms, which is in agreement with previous FO's result. However, ELF cannot clarify the bond energy composition; it should be elucidated by EDA as follow section.

3.3. Energy decomposition analysis

To get a more detailed insight into the nature of the M–M bond in alkaline-Earth dimetallocene complexes, an energy decomposition analysis (EDA) has been carried out. Table 3 collects the results of the EDA for $M_2\text{–}(\eta^5\text{–}C_5H_5)_2$ (M = Be, Mg, Ca, Sr and Ba) using M(Cp) ligand as fragments. The M–M bond dissociation energy (D_e) derived from the EDA calculations follow a trend Ba < Sr < Ca < Mg < Be, which is lower than that in $Zn_2(\eta^5\text{–}C_5H_5)_2$ we have reported. The similar trend is observed for the interaction energy (ΔE_{int}). The results reveal that the Be and Mg compounds are more stable than Sr and Ba compounds. The significantly weaker CpBa–BaCp bond can be explained with the small electrostatic and orbital contributions to the bonding. Obviously, the values of ΔE_{Pauli}, ΔE_{elstat} and ΔE_{orb} for Group 2 dimetallocene complexes show markedly monotonic rules from Be to Ba, and is similar to the trend observed for ΔE_{int} and D_e values. Note that the absolute values of ΔE_{Pauli}, ΔE_{elstat} and ΔE_{orb} for the beryllium complex are much larger than for the other alkaline-Earth metal homologues. The comparison of the EDA data for Group 2 dimetallocene complexes with the values for Zn_2Cp_2 indicates that ΔE_{Pauli} term is smaller than that in Zn_2Cp_2, especially for Ca, Sr and Ba compounds.

Xie et al. predicted by NBO analysis that, in dimetallocene, it forms covalent bond between two metal fragments (Be, Mg or Ca), and a predominantly ionic bond between metal and cyclopentadienyl ring [21]. Green et al. also indicate that it has single covalent Mg–Mg interaction in the novel thermally stable magnesium(I) compounds. It is interesting to clarify if M–M bond would be really pure covalent bonding [23]. The data collected in Table 3 show that the ΔE_{elstat} term yields 50.2–64.9% of the total attractive forces from Be_2Cp_2 to Ba_2Cp_2. The electrostatic character of the bonding in Be complexes is slightly larger (64.9%) than in

Table 2
BP86 HOMO molecular orbital component (%) from alkaline-Earth metal in $M_2\text{–}(\eta^5\text{–}C_5H_5)_2$ (M = Be, Mg, Ca, Sr, Ba) with TZP, TZ2P and QZ4P basis sets.

	Be			Mg			Ca			Sr			Ba		
	2s	$2p_z$	$3dz^2$	3s	$3p_z$	$3dz^2$	4s	$4p_z$	$3dz^2$	5s	$5p_z$	$4dz^2$	6s	$6p_z$	$5dz^2$
TZP	75.1	19.6	0	81.3	15.7	0	82.1	10.1	5.7	82.2	11.7	4.7	75.6	10.6	12.6
TZ2P	76.6	20.6	0	80.8	16.4	0	79.6	11.7	7.2	81.6	12.3	4.9	75.6	11.7	12.6
QZ4P	66.7	26.0	0	79.6	15.7	0	73.2	17.6	7.1	78.1	15.1	5.5	73.7	9.2	15.0

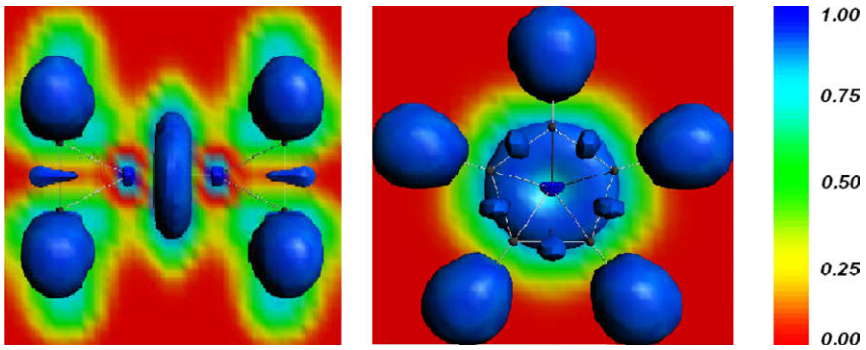

Fig. 3. Electron localization function of $Be_2(\eta^5\text{–}C_5H_5)_2$ with a plotted isosurface value of 0.96. M–M axis direction (left) and perpendicular direction (right).

Table 3
Energy decomposition analysis (kcal/mol) of the $M_2\text{–}(\eta^5\text{–}C_5H_5)_2$ (M = Be, Mg, Ca, Sr, Ba and Zn) at the BP86/TZ2P level of theory using M(Cp) ligand as fragments.

Term	CpBeBeCp	CpMgMgCp	CpCaCaCp	CpSrSrCp	CpBaBaCp	CpZnZnCp [24]
ΔE_{int}	−68.95	−45.70	−28.21	−22.85	−16.07	−71.10
ΔE_{Pauli}	46.47	24.38	12.52	13.06	9.18	68.99
ΔE_{elstat}	−74.95 (64.9%)[a]	−41.63 (58.8%)	−21.45 (51.9%)	−20.39 (56.8%)	−12.68 (50.2%)	−85.99 (61.4%)
ΔE_{orb}	−40.47 (35.1%)	−28.45 (41.2%)	−19.28 (48.1%)	−15.51 (43.2%)	−12.57 (49.8%)	−54.09 (38.6%)
a_1	−39.14	−28.31	−19.29	−15.54	−12.65	−52.20
a_2	0.00	0.00	0.00	0.00	0.00	0.00
e_1	−1.18	−0.14	0.02	0.03	0.08	−1.90
e_2	−0.16	−0.01	−0.02	0.00	0.00	0.02
ΔE_σ	−39.14	−28.31	−19.29	−15.54	−12.65	−52.20
ΔE_π	−1.18	−0.14	0.02	0.03	0.08	−1.90
ΔE_{prep}	1.40	1.16	0.40	0.04	0.0	0.40
$\Delta E(-D_e)$	−67.55	−44.54	−27.81	−22.81	−16.07	−70.70
q(M)	0.834	0.878	0.864	0.884	0.894	0.914

[a] The value in parentheses gives the percentage contribution to the total attractive interactions ($\Delta E_{elstat} + \Delta E_{orb}$).

other group 2 metal compounds (50.2–58.8%). Therefore, the M–M bonding in alkaline-Earth dimetallocene complexes have more ionic than covalent character (ΔE_{orb}), especially in Be species. With the exception of Be compound, there are higher covalent character for the alkaline-Earth dimetallocene complexes than for the zinc homologue. Comparison of the EDA results of $Zn_2(Cp)_2$ with those of the alkaline-Earth dimetallocenes gives information that the transition metal Zn behaves more as a main-group element in +1 oxidation state compounds.

The decomposition of ΔE_{orb} into contributions from the different symmetry representations of the C_{5v} point group shows that the largest contribution to the covalent bonding comes from the a_1 (σ) interaction, while the contribution of the e_1 (π) orbital is much smaller and is negligible. The δ (e_2 irreducible representation) orbital interaction of M–M is almost vanished, which is agreement with results of molecular orbital analysis.

The metal–Cp interactions in metallocene have been investigated greatly with quantum chemical calculations in recent years. Table 4 gives also the results of the bonding analysis of dimetal–ligand interaction. The EDA results suggest that the bonding interactions between M_2^{2+} and $(Cp^-)_2$ have a larger electrostatic than covalent character, particularly for the Mg, Ca, Sr and Ba compounds. The diberyllocene is a bit more covalently bonded than the other species, but the percentage contribution of ΔE_{elstat} to the total attraction is still higher (61%) than the contribution of ΔE_{orb}. The values are in excellent agreement with results of Merino et al. [22]. The EDA results of Sr and Ba dimetallocene presented here are theoretical studied for the first time. The NBO atomic partial charges for metal, ca. ~+0.9, supports the predominantly ionic in metal–ligand interactions. However, the sequence of charge for metal is not in accordance with that in energy term ΔE_{elstat} and ΔE_{int}. So it is important to note

Table 4
Energy decomposition analysis (kcal/mol) of the $M_2\text{–}(\eta5\text{–}C_5H_5)_2$ (M = Be, Mg, Ca, Sr, Ba) at the BP86/TZ2P level of theory using $2Cp^-$ ligand and M_2^{2+} as fragments.

Term	Be_2Cp_2	Mg_2Cp_2	Ca_2Cp_2	Sr_2Cp_2	Ba_2Cp_2
ΔE_{int}	−669.66	−510.32	−448.78	−415.83	−392.95
ΔE_{Pauli}	96.93	90.33	125.42	129.20	164.03
ΔE_{elstat}	−470.44 (61.3%)	−452.83 (75.4%)	−435.95 (75.9%)	−422.49 (77.5%)	−428.18 (76.9%)
ΔE_{orb}	−296.15 (38.7%)	−147.82 (24.6%)	−138.25 (24.1%)	−122.54 (22.5%)	−128.80 (23.1%)
a'_1	−48.88	−28.27	−30.01	−26.09	−31.95
a'_2	0.00	0.00	0.00	0.00	0.00
e'_1	−96.50	−40.80	−42.24	−37.95	−39.51
e'_2	−11.70	−7.77	−5.59	−4.97	−4.38
a''_1	0.00	0.00	0.00	0.00	0.00
a''_2	−44.83	−24.51	−12.89	−11.48	−10.42
e''_1	−82.58	−38.68	−41.92	−37.08	−38.16
e''_2	−11.65	−7.78	−5.59	−4.97	−4.38

that atomic partial charges cannot be taken as a measure criterion of the electrostatic interactions.

4. Summary and conclusion

In this contribution, we have carried out quantum chemical calculations on the structure and bonding nature between containing Group 2 elements in the dimetallocene sandwich complexes CpM–MCp (M = Be–Ba). Molecular orbital results reveal that, for the heavier alkaline-Earth metal (Ca, Sr and Ba) compounds, substantial $(n-1)$d character is found in the bonding between metal and Cp ring, while there is few δ bonding interaction between M–M bond due to longer M–M bond distance. The calculated bond dissociation energies of the Group 2 dimetallocene complexes exhibit the trend: Be > Mg > Ca > Sr > Ba. Diberyllocene has clearly the strongest metal–metal bonds among the Group 2 complexes ($D_e = -67.55$ kcal mol^{-1}), which is close to Zn species ($D_e = -70.7$ kcal mol^{-1}). From the quantitative bond energy decomposition, the natures of M–M bonding of Group 2 elements are assessed. Inspection of the various energy terms which contribute to interaction energy ΔE_{int} indicates that the M–M binding interactions in all complexes have more ionic character than covalent character, rather than the sole covalent bond character; this is revealed by the percentage values for ΔE_{elstat} (50.2–64.9%). The substantial covalent character of metal–metal bond in these complexes comes mainly from $a_1(\sigma)$ orbital interactions, which gains substantial stabilization from predominantly the <*ns*|*ns*> bond. The electrostatic attraction is an important component in present studied homodinuclear transition metal complexes.

Acknowledgments

This work was financially supported by the China NSF (Grant Nos. 20703008, 20671038) and the Natural Science Foundation of Jiangsu Educational Office (No. 06KJD150031), and the Opening Project of Key Laboratory for Chemistry of Low-Dimensional Materials of Jiangsu Province (No. JSKC06032).

References

[1] P. Jutzi, Chem. Rev. 86 (1986) 983.
[2] P. Jutzi, N. Burford, Chem. Rev. 99 (1999) 969.
[3] D.J. Burkey, T.P. Hanusa, Comm. Inorg. Chem. 17 (1995) 41.
[4] P. Jutzi, N. Burford, in: A. Togni, T.P. Hanusa (Eds.), Metal–metal bonding in alkaline-Earth metallocenes, Wiley-VCH, 2005. Chapter 1.
[5] I. Resa, E. Carmona, E. Gutierrez-Puebla, A. Monge, Science 305 (2004) 1136.
[6] Z.Z. Liu, W.Q. Tian, J.K. Feng, G. Zhang, W.Q. Li, THEOCHEM 758 (2006) 127.
[7] S.L. Richardson, T. Baruah, M.R. Pederson, Chem. Phys. Lett. 415 (2005) 141.
[8] Z.Z. Xie, W.H. Fang, Chem. Phys. Lett. 404 (2005) 212.
[9] Y.M. Xie, H.F. Schaefer, R.B. King, J. Am. Chem. Soc. 127 (2005) 2818.
[10] D. del Rio, A. Galindo, I. Resa, E. Carmona, Angew. Chem. Int. Ed. 44 (2005) 1244.
[11] J.W. Kress, J. Phys. Chem. A 109 (2005) 7757.
[12] H.M. Wang, C.L. Yang, B.S. Wan, K.L. Han, J. Theor. Comput. Chem. 5 (2006) 461.
[13] H.Z. Xiu, L. Se, S.L. Qian, J. Theor. Comput. Chem. 5 (2006) 475.
[14] Z.Z. Liu, W.Q. Tian, J.K. Feng, G. Zhang, W.Q. Li, Y.H. Cui, C.C. Sun, Eur. J. Inorg. Chem. (2006) 2808.
[15] M.R. Philpott, Y. Kawazoe, THEOCHEM 773 (2006) 43.
[16] M.R. Philpott, Y. Kawazoe, Chem. Phys. 327 (2006) 283.
[17] T.P. Hanusa, Organometallics 21 (2002) 2559.
[18] T.P. Hanusa, Chem. Rev. 93 (1993) 1023.
[19] R. Fernandez, E. Carmona, Eur. J. Inorg. Chem. (2005) 3197.
[20] V.M. Rayon, G. Frenking, Chem. Eur. J. 8 (2002) 4693.
[21] Y.M. Xie, H.F. Schaefer, E.D. Jemmis, Chem. Phys. Lett. 402 (2005) 414.
[22] A. Velazquez, I. Fernandez, G. Frenking, G. Merino, Organometallics 26 (2007) 4731.
[23] S.P. Green, C. Jones, A. Stasch, Science 318 (2007) 1754.
[24] Y.H. Kan, THEOTHEM 805 (2007) 127.
[25] E. Vanlenthe, E.J. Baerends, J.G. Snijders, J. Chem. Phys. 101 (1994) 9783.
[26] G.T. Velde, F.M. Bickelhaupt, E.J. Baerends, C.F. Guerra, S.J.A. Van Gisbergen, J.G. Snijders, T. Ziegler, J. Comput. Chem. 22 (2001) 931.
[27] J. Poater, M. Duran, M. Sola, B. Silvi, Chem. Rev. 105 (2005) 3911.
[28] M. Kohout, program DGrid, version 4.1, Max-Planck Institut für Chemische Physik fester Stoffe, Dresden, 2006.
[29] M. Westerhausen, M. Gärtner, R. Fischer, J. Langer, L. Yu, M. Reiher, Chem. Eur. J. 13 (2007) 6292.
[30] A.J. Bridgeman, C.J. Empson, Chem. Eur. J. 12 (2006) 2252.
[31] L. Gagliardi, P. Pyykkö, Theor. Chem. Acc. 110 (2003) 205.